

Effect of Hydrogen Addition on the Flammability Limit of Stretched Methane/Air Premixed Flames

Ramanan Sankaran and Hong G. Im *
Department of Mechanical Engineering
University of Michigan
Ann Arbor, MI 48109

Abstract

A computational study is performed to investigate the effects of hydrogen addition on the fundamental characteristics of stretched methane/air premixed flame in an opposed flow configuration. The problem is of interest as a potential application to gas turbines and spark-ignition engines, where it has been anticipated that addition of a small amount of hydrogen will extend the lean flammability limit, allowing combustion at leaner conditions to achieve lower NO_x emission. The flame response is first studied under steady conditions with different levels of hydrogen addition. The results show that the extinction strain rate and the lean flammability limit are significantly extended due to the presence of hydrogen in the mixture. On the other hand, the consumption speed and time scale of the flame close to extinction were found to be insensitive to the extent of blending. Further simulations were performed in an unsteady opposed-flow configuration to study the effects of mixture stratification at various time scales. The dependence of the dynamic flammability limits on the mean composition was determined at various frequencies and compared with a pure methane-air flame.

Introduction

In many practical applications for power generation, such as gas turbines, there has been strong interest in achieving lean premixed combustion. The advantages of operating at very lean mixture conditions are high thermal efficiency and low emissions of NO_x due to lower flame temperatures. However, operating very close to the lean flammability limit has the drawback of local extinction, emissions of unburnt hydrocarbons, and large-amplitude oscillations in pressure that can result in mechanical damage [1]. These considerations demand the mixture to be significantly richer than what would otherwise be desirable. It has been shown in earlier studies that blending of hydrogen with hydrocarbon fuels improves its lean flammability limit and flame propagation speed [2, 3, 4], thereby enabling stable combustion at lean mixture conditions. In the case of natural gas engines, enriching the fuel with hydrogen has the proven benefits of improving the combustion stability and reducing the emissions [5, 6, 7]. The available results indicate a definite advantage in blending hydrogen, provided an economical and efficient source of hydrogen can be established.

In this paper, we study the effects of hydrogen addition on stretched premixed methane-air flames. It is known from earlier studies [2, 3, 4] that blending of hydrogen causes an increase in the laminar flame speed (S_L) of a freely propagating flame due to an increase in the flame temperature (thermal effect) and an increased supply of active radicals (chemical effect). In a more recent work that considered the effect of strain rate [8], Ren *et al.* concluded that the increase in extinction strain rate due to hydrogen addition outweighs

the effects on flame speed and flammability limit. The primary objective of this paper is to quantify the increased immunity of lean premixed flames to flow strain due to the blending of hydrogen. In particular, the mixing between diffusive-thermally neutral methane and highly diffusive hydrogen can introduce unique dynamic behavior of stretched premixed flames.

Another focus of the study is the basic characteristics of premixed combustion in an inhomogenous mixture field. Due to the lack of understanding of the flame response under a spectrum of various mixture composition due to the initial stratification and subsequent turbulent mixing process, several earlier simulations of the direct injection spark ignition (DISI) engine have relied on empirical assumptions for the combustion models [9, 10, 11]. In the last symposium [12], we demonstrated that a stretched flame with transient composition fluctuation is able to sustain combustion even if the equivalence ratio temporarily becomes lower than the steady flammability limit for a certain duration of time. This observation is further examined in the present study by exploring the effect of mixture stratification in a system with multi-component fuels and the dependence of the dynamic flammability limit on the characteristic time scale of the flame.

Formulation and Numerical Method

The computational configuration is a counterflow premixed flame between two opposing axisymmetric nozzles separated by a distance L . The governing equations for this configuration and details of the numerical implementation can be found in Ref. [13]. The steady solutions are obtained using a modified version of OPPDIF [14] and the unsteady solutions using OPUS [15]. These codes are interfaced with

*Corresponding author: hgim@umich.edu
Proceedings of the Third Joint Meeting of the U.S. Sections of The Combustion Institute

Chemkin [16] and Transport [17]. The full methane-air kinetic mechanism (GRI 3.0) [18] including NO_x chemistry has been used. The radiative heat transfer term is included by using the optically-thin gas approximation, where the Planck mean absorption constants are taken from Ju *et al.* [19].

To understand the strained premixed flame characteristics, a symmetric back-to-back premixed flame is established by supplying premixed fuel-air mixture at identical conditions from both nozzles. Only a half of the domain is actually solved by applying the symmetry boundary condition at the stagnation plane. A zonal grid refinement method is used to capture the flame moving in the computational domain [13]. The grid convergence is fully tested to ensure the numerical accuracy of the solutions.

The reactant stream consists of a premixed CH₄-H₂-air mixture. The temperature at the inlet is set to 300K and the pressure is 1 atm for all the test cases. Due to the presence of multiple fuels in the mixture, it is necessary to suitably define the equivalence ratio such that it takes into account the overall stoichiometry of the mixture. Following Yu *et al.* [2], we define two parameters, ϕ and R_H , characterizing the effective equivalence ratio and extent of hydrogen blending respectively, namely

$$\phi = \frac{C_F / [C_A - C_H / (C_H / C_A)_{st}]}{(C_F / C_A)_{st}}, \quad (1)$$

$$R_H = \frac{C_H + C_H / (C_H / C_A)_{st}}{C_F + [C_A - C_H / (C_H / C_A)_{st}]}, \quad (2)$$

in which C_F , C_H , and C_A are the mole fractions of methane, hydrogen and air, respectively. The subscript ‘st’ denotes the stoichiometric conditions. The above definitions imply that hydrogen is always completely oxidized and only the remaining air is used to oxidize methane. The effective equivalence ratio ϕ of methane is defined in Eq. (1) based on this assumption. Also, in Eq. (2), the numerator is the amount of hydrogen plus the stoichiometric amount of air to completely consume hydrogen, while the denominator is the amount of methane plus the amount of air available for its oxidation. These two parameters have been shown to be a reasonable choice for data reduction and correlation [2]. We first study the effect of hydrogen blending on a steady flame at various mixture conditions.

Steady Stretched Flame Response

The response of a steady methane-air flame at $\phi = 0.7$ is computed with different levels of hydrogen addition. Figure 1 shows the variation of the maximum flame temperature (at the symmetry boundary), T_b , as a function of the imposed strain rate for a pure methane-air flame ($R_H = 0$) and with two levels of hydrogen addition ($R_H = 0.05, 0.1$). For these values of R_H , the ratio of the mole fractions of H₂ to the total mole fraction of the fuel ($C_H / (C_F + C_H)$) is roughly 18% and 30% respectively. Also, the strain rate (κ) is de-

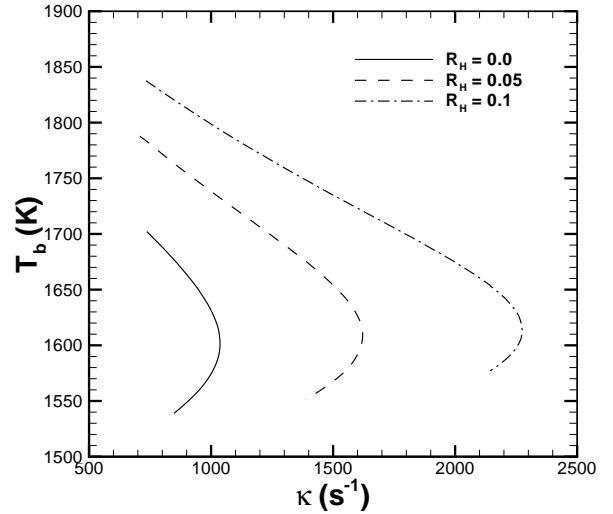


Figure 1: Flame Temperature variation with strain rate at $\phi=0.7$.

finned as the radial velocity gradient at the location of maximum heat release. In all the cases, T_b decreases monotonically with increasing strain rate, until the extinction point is reached. The extinction strain rates at $R=0.0, 0.05, 0.1$ are $\kappa_{ext}=1040, 1620$ and 2270 s^{-1} , respectively, demonstrating an increased immunity to stretch driven extinction with hydrogen addition. This can result in a significant improvement in the operation of lean burn gas turbines.

We further investigate the variation of the flame speed, which represents the overall rate of combustion. The consumption speed has been found to be a reasonable measure of the burning velocity of a stretched flame even under unsteady conditions [20]. The consumption speed based on a species k is defined as [21]

$$S_c = \frac{W_k \int \omega_k d\eta}{\rho_u (Y_{k,b} - Y_{k,u})}, \quad (3)$$

where subscripts ‘u’ and ‘b’ denote the unburnt and burnt sides, respectively, W_k is the molecular weight of species k , and ω_k is its molar reaction rate. Figure 2 shows the variation of consumption speed based on methane for the above cases. Note that, unlike the response of T_b , the consumption speed initially increases with strain rate and then starts decreasing at a point much earlier than extinction. Based on the diffusive properties of the unburnt mixture, the effective Lewis number is estimated to be 0.96. In general, the methane-air mixture is considered nearly equidiffusive, hence the nonmonotonic behavior of the consumption speed cannot be explained based on the Lewis number effect.

To substantiate this point, Fig. 3 shows the normalized

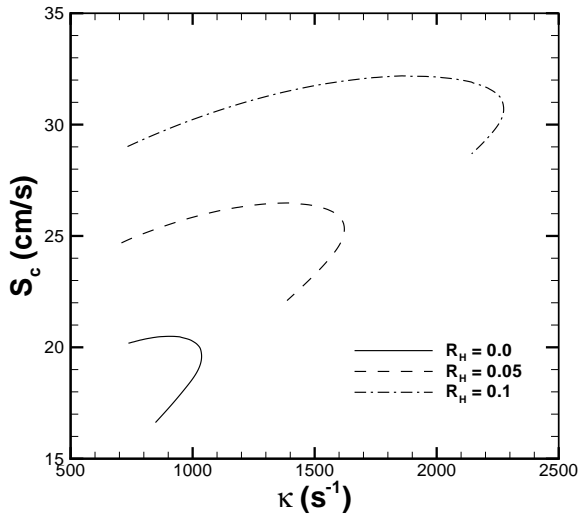


Figure 2: Variation of consumption speed with strain rate at $\phi = 0.7$.

consumption speed and the mass fraction of methane at the stagnation plane ($Y_{CH_4,b}$) are plotted against κ . S_c has been normalized using the corresponding laminar flame speeds, which is 20, 24 and 28 cm/s for $\phi=0.7$, $R_H = 0.0, 0.05$ and 0.1 respectively [2]. As κ increases, S_c increases and the flame moves closer to the stagnation plane. At a critical strain rate, κ_c , defined as the strain rate at which the reaction layer attaches to the stagnation plane, the amount of unburnt reactant increases rapidly, which is evident from the increase in CH_4 mass fraction at the burnt side (see Fig. 3). This leads to a decrease in the reaction rate and eventually extinction. This suggests that the decrease in S_c near extinction is a confinement effect due to the downstream interaction, and for lower strain rates the consumption speed appears to increase with an increase in strain rate. This issue is being investigated for clear explanation.

Unlike S_c , the temperature of the flame decreases monotonically, which can be explained by visualizing the reaction zone as having a thin inner reaction layer and a downstream CO oxidation layer [22]. While the flame temperature continuously decreases due to the incomplete oxidation of CO, the effect is not felt by the consumption speed until the inner reaction layer reaches the stagnation plane. It is also seen from Fig. 3 that addition of hydrogen causes a substantial increase in the burning velocity, even in the presence of stretch, both in absolute terms and relative to their laminar flame speeds.

One could possibly argue that the blending of hydrogen may also affect the equidiffusive nature of the methane-air flame. While Joulin and Mitani [23] have derived an expres-

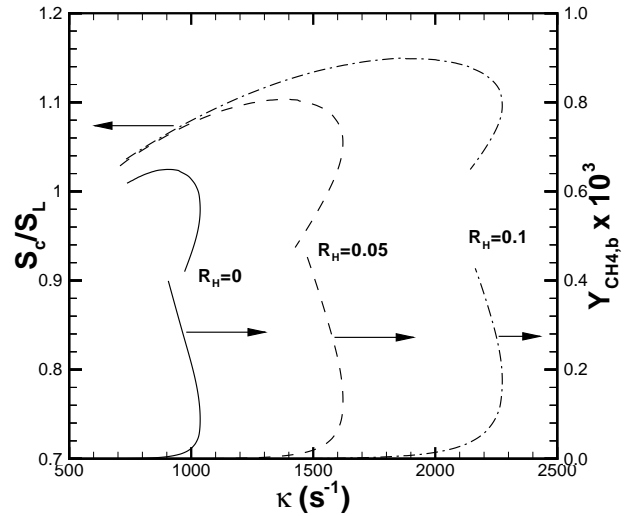


Figure 3: Normalized consumption speed and reactant leakage as a function of strain rate.

sion for the effective Lewis number for two-reactant near-stoichiometric flames, it is difficult to accurately estimate the effective Lewis number of a multi-component fuel mixtures. We estimate the effect of hydrogen blending on Lewis number using the available strain rate data as follows.

Sun and Law [24] have derived the analytical expressions characterizing the extinction of a counterflow flame due to incomplete reaction using an integral analysis. In our results, the amount of unburnt fuel at the stagnation plane increases exponentially (see Fig. 3), which is in good agreement with the analytical prediction. According to the results of their integral analysis, the ratio of the critical strain rate (κ_c) to the extinction strain rate (κ_{ext}) is given by

$$\ln \left(\frac{\kappa_c}{\kappa_{ext}} \right) = \ln Le + Le - 1. \quad (4)$$

The results of the Lewis number calculated using Eq.(4) are shown in Table 1. The critical strain rate was defined as the point where the unburnt reactant mass fraction exceeds 1×10^{-5} , which coincides with the point of peak consumption speed. The addition of hydrogen does reduce the Lewis number of the mixture. However, at the levels of blending considered, it is not substantial enough to alter the equidiffusive behavior.

Next we study the variation of the flame temperature, T_b , as a function of the equivalence ratio, at a fixed strain rate of $\kappa=1100 \text{ s}^{-1}$. As is seen from Fig. 4, the flame temperatures decrease as the mixture equivalence ratio decreases, and eventually reach the limit beyond which no steady com-

Table 1: Estimated Lewis number based on κ_c and κ_{ext}

R_H	$\kappa_c(\text{s}^{-1})$	$\kappa_{ext}(\text{s}^{-1})$	Le
0	950	1040	0.9552
0.05	1430	1620	0.9385
0.1	1950	2270	0.9255

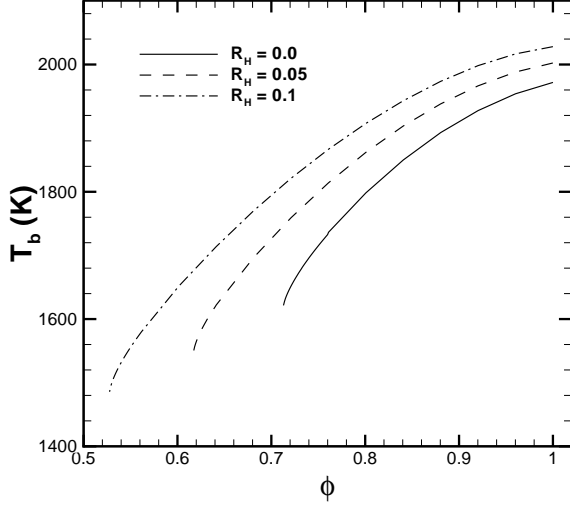


Figure 4: Flame temperature as a function of equivalence ratio at a fixed strain rate, $\kappa=1100\text{s}^{-1}$.

bustion can exist. The steady flammability limit¹, ϕ_s^* , is defined as the minimum equivalence ratio for a steady stretched flame to exist, and is a function of the imposed strain rate. For the conditions shown in Fig. 4, the flammability limits are found to be $\phi_s^* = 0.712$, 0.617 and 0.527 at $R_H = 0$, 0.05 and 0.1 respectively. The advantages of blending hydrogen are two-fold – the ability to sustain combustion at a much leaner mixture condition, and secondly, the lower flame temperature close to the flammability limit. In other words, although the temperature of a blended flame is higher than a pure methane-air flame of the same equivalence ratio, by taking the advantage of the extended flammability limit it is possible to burn at a lower temperature, which might lead to lower NOx emissions.

The variation of the consumption speed (S_c) for the same set of cases, as a function of the equivalence ratio is plotted in Fig. 5. It is readily seen that, despite the differences in the value of ϕ_s^* , the consumption speed at and near the extinction point is similar for all the cases. This has a sig-

¹Although the conventional “flammability limit” is defined for unstrained premixed flames and thus should be independent of strain rate, we choose to extend this terminology for a strained flame as well, since we are concerned about a critical mixture composition.

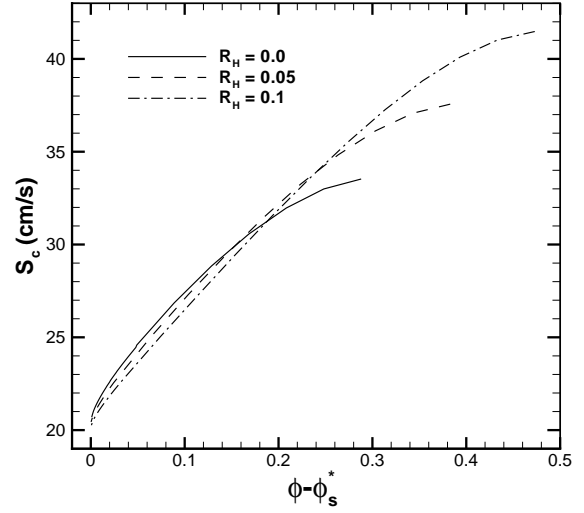


Figure 5: Consumption speed as a function of equivalence ratio at a fixed strain rate, $\kappa=1100\text{s}^{-1}$.

nificance in considering the characteristic flame time scale (t_F), which can be defined as $t_F = \frac{D}{S_c^2}$, where D is the average diffusivity of the fuel species. Also, the consumption speed, S_c , has been demonstrated to be a good measure of the propagation speed of the flame front [20]. The results in Fig. 5 and the above definition imply that at a fixed strain rate, the characteristic flame time scale is almost insensitive to blending. This conjecture is confirmed by the results obtained using an oscillatory composition at the inlet.

Unsteady Response to Composition Fluctuations

In our earlier study [12] on the response of a stretched premixed flame to time-varying compositions, it was reported that the flame can be sustained at equivalence ratios lower than the steady flammability limit, when the time scales of the fluctuations are comparable to those of the flame. To study the effect of composition fluctuation, the velocity at the inlet is held fixed and the equivalence ratio ϕ is varied in time. We use a monochromatic oscillation of the form,

$$\phi(t) = \phi_0[1 - A(1 - \cos(2\pi ft))]. \quad (5)$$

The effect of oscillations in R_H was not considered. Since hydrogen is a highly diffusive species, any spatial variation in its composition is expected to diffuse out faster than methane, hence is unlikely to change the results significantly.

Figure 6 shows some typical unsteady flame response in the case of $\kappa=1100\text{s}^{-1}$ and $R_H=0$, where the flame temperature, and the consumption speed are plotted versus the instantaneous mixture equivalence ratio, evaluated at the flame

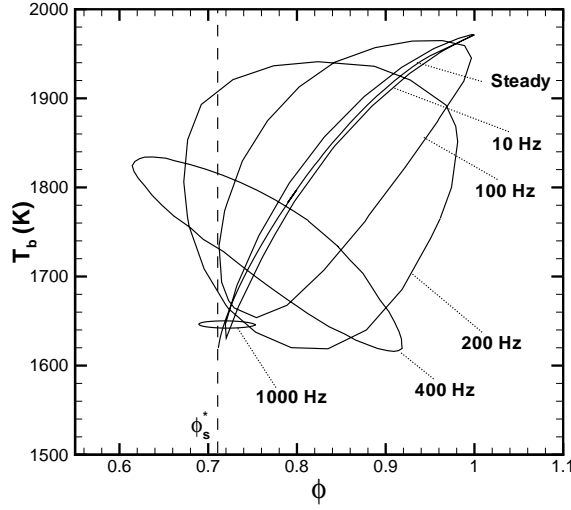


Figure 6: Response of flame temperature to the oscillatory equivalence ratio at flame base

base, once the limit cycle is reached. For all the cases shown, $\phi_0=1$ and the amplitude is taken to be the maximum value that can be reached without extinguishing the flame. The results show that the flame can self-sustain at higher frequencies even if the equivalence ratio falls below the steady flammability limit ϕ_s^* for some part of the cycle. This led us to define a dynamic flammability limit, ϕ_t^* , as the minimum allowable equivalence ratio for unsteady flames. A parametric mapping of the dependence of ϕ_t^* on the strain rate (κ), mean composition ($\bar{\phi}$) and frequency of oscillation (f) has been presented in Ref. [12].

In this paper, we determine the dynamic flammability limits of methane-air flame with hydrogen blending and compare it with the corresponding limits of an unblended fuel. The results for $R_H = 0.05$ and 0.1 compared with a pure methane-air flame is shown in Fig. 7. The functional relationship between the dynamic flammability limit and the mean composition seems to be independent of the extent of hydrogen blending, as can be explained by the following analysis. The flame response at any time can be considered to depend not on the instantaneous state of the mixture composition, but rather on the history of its variation [25]. Therefore, at any instant of time, the behavior of the flame is governed by the integral of the mixture condition over the characteristic flame time scale (t_F) instead of its instantaneous value. This integral quantity is written as

$$\phi_I(t) = \int_{t-t_F}^t \phi(t) dt. \quad (6)$$

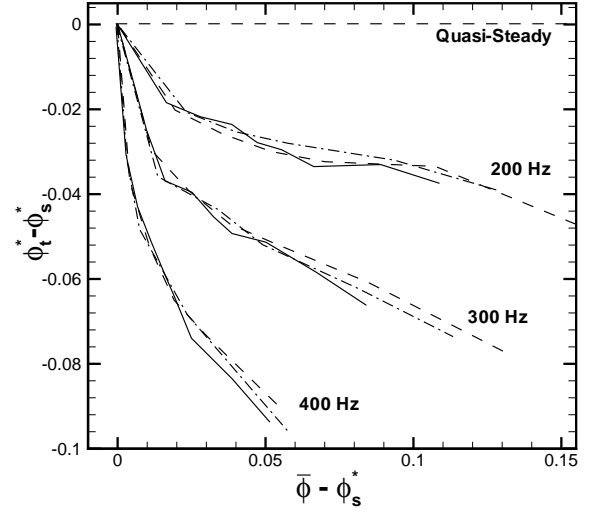


Figure 7: Dynamic flammability limits as a function of the mean equivalence ratio for various levels of hydrogen blending; $R=0$ (—), $R=0.05$ (---) and $R=0.1$ (- · - · -).

Given that $\phi(t) = \bar{\phi} + A \sin(2\pi ft)$, Eq. (6) yields,

$$\phi_I(t) = \bar{\phi} + \frac{A \sin(\pi f t_F)}{\pi f t_F} \sin \left[2\pi f \left(t - \frac{t_F}{2} \right) \right]. \quad (7)$$

The flammability criterion based on the steady limit (ϕ_s^*) would demand that $\phi_{I,\min} \geq \phi_s^*$, which yields

$$(\phi_t^* - \phi_s^*) = (\bar{\phi} - \phi_s^*) \left[1 - \frac{\pi f t_F}{\sin(\pi f t_F)} \right]. \quad (8)$$

Figure 8 shows the analytical solution obtained using the above equation, where the time scale $t_F = D/S_c^2(\bar{\phi})$, $D=1.0$ cm^2/s , and S_c was extracted from Fig. 5. Although Eq. (8) cannot match the exact magnitude of the dynamic flammability limits, it does a good job in predicting the qualitative trend. The agreement between the results for various levels of blending seen in Fig. 7 supports our conclusion that blending of hydrogen does not affect the time scale of the flame close to the flammability limit. Furthermore, the ability of Eq. (8) to qualitatively predict the trends of the dynamic flammability limit demonstrates the relevance of the flame consumption speed, S_c , in determining the flame time scale.

Conclusions

The effects of hydrogen blending on a stretched methane-air premixed flame has been computationally studied. The results demonstrated an increased extinction strain rate and lower lean flammability limits due to the addition of hydrogen. Furthermore, the effect of hydrogen addition on the

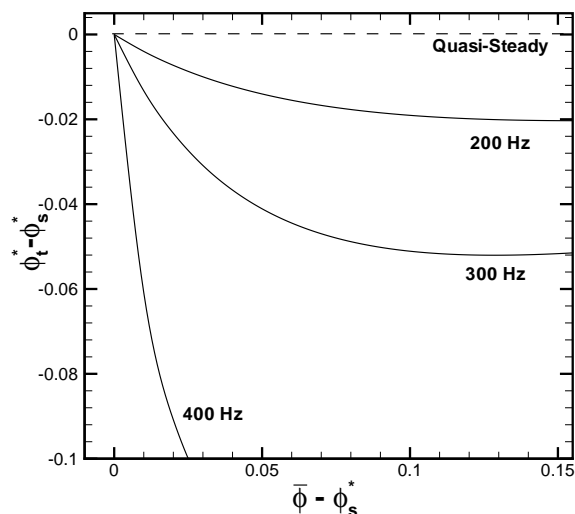


Figure 8: Analytical solution for the dynamic flammability limits obtained using Eq. (8).

Lewis number of the flame was estimated and found to be insignificant for the cases studied. At a fixed strain rate, the consumption speed of the flame close to extinction was invariant even with blending. Unsteady simulations to study the effect of mixture stratification led to similar results for the dynamic flammability limits as a pure methane-air flame.

Acknowledgement

This work was supported by Sandia National Laboratories, Livermore, CA, under the contract through the Combustion Research Facility.

References

- De Zilwa, S. R. N., Uhm, J. H., and Whitelaw, J. H. *Combust. Sci. Tech.* 160:231–258 (2000).
- Yu, G., Law, C. K., and Wu, C. K. *Combust. Flame* 63:339–347 (1986).
- Sung, C. J., Huang, Y., and Eng, J. A. *Combust. Flame* 126:1699–1713 (2001).
- Gauducheau, J. L., Denet, B., and Searby, G. *Combust. Sci. Tech.* 137:81–99 (1998).
- Allenby, S., Chang, W.-C., Megaritis, A., and Wyszynski, M. L. *Journal of Automobile Engineering* 215:405–418 (2001).
- Bade Shrestha, S. O. and Karim, G. A. *Int. J. Hydrogen Energy* 24:577–586 (1999).
- El-Sherif, S. A. *Fuel* 79:567–575 (2000).
- Ren, J.-Y., Qin, W., Egolfopoulos, F. N., and Tsotsis, T. T. *Combust. Flame* 124:717–720 (2001).
- Gill, A., Gutheil, E., and Warnatz, J. *Combust. Sci. Tech.* 115:317–333 (1996).
- Baritaud, T. A., Duclos, J. M., and Fusco, A. *Proc. Combust. Inst.* 26:2627–2635 (1996).
- Helie, J., Duclos, J. M., Baritaud, T., Poinso, T., and Trouve, A. *SAE Technical Paper* 2001-01-1226 (2001).
- Sankaran, R. and Im, H. G. *Proc. Combust. Inst.* 29 (2002).
- Im, H. G., Raja, L. L., Kee, R. J., and Petzold, L. R. *Combust. Sci. Tech.* 158:341–363 (2000).
- Lutz, A. E., Kee, R. J., Grcar, J. F., and Rupley, F. M. *OPPDIF: A Fortran Program for Computing Opposed-Flow Diffusion Flames*. Tech. Rep. SAND96-8243, Sandia National Laboratories (1997).
- Im, H. G., Raja, L. L., Kee, R. J., Lutz, A. E., and Petzold, L. R. *OPUS: A Fortran Program for Unsteady Opposed-Flow Flames*. Tech. Rep. SAND2000-8211, Sandia National Laboratories (2000).
- Kee, R. J., Rupley, F. M., and Miller, J. A. *Chemkin-II: A Fortran Chemical Kinetics Package for the Analysis of Gas-Phase Chemical Kinetics*. Tech. Rep. SAND89-8009B, Sandia National Laboratories (1991).
- Kee, R. J., Dixon-Lewis, G., Warnatz, J., Coltrin, M. E., and Miller, J. A. *A Fortran Computer Code Package for the Evaluation of Gas-Phase Multicomponent Transport Properties*. Tech. Rep. SAND86-8246, Sandia National Laboratories (1986).
- Smith, G. P., Golden, D. M., Frenklach, M., *et al.* http://www.me.berkeley.edu/gri_mech/.
- Ju, Y., Guo, H., Maruta, K., and Liu, F. *J. Fluid Mech.* 342:315–334 (1997).
- Im, H. G. and Chen, J. H. *Proc. Combust. Inst.* 28:1833–1840 (2000).
- Poinso, T., Echekki, T., and Mungal, G. *Combust. Sci. Tech.* 81:45–73 (1992).
- Peters, N. In W. A. Sirignano, A. G. Merzhanov, and L. D. Luca, eds., *Advances in Combustion Science: In Honor of Ya. B. Zel'dovich*, vol. 173 of *Progress in Astronautics and Aeronautics*, pp. 73–91 (1997).
- Joulin, G. and Mitani, T. *Combust. Flame* 40:235–246 (1981).
- Sun, C. J. and Law, C. K. *Combust. Flame* 121:236–248 (2000).
- Lauvergne, R. and Egolfopoulos, F. N. *Proc. Combust. Inst.* 28:1841–1850 (2000).